Helical Conformation of the SEVI Precursor Peptide $PAP_{248-286}$, a Dramatic Enhancer of HIV Infectivity, Promotes Lipid Aggregation and Fusion

Jeffrey R. Brender,[†‡*] Kevin Hartman,[†] Lindsey M. Gottler,[†‡] Marchello E. Cavitt,[†] Daniel W. Youngstrom,[‡] and Ayyalusamy Ramamoorthy[†‡*]

[†]Department of Chemistry and [‡]Department of Biophysics, University of Michigan, Ann Arbor, Michigan

ABSTRACT In previous in vivo studies, amyloid fibers formed from a peptide ubiquitous in human seminal fluid (semen-derived enhancer of viral infection (SEVI)) were found to dramatically enhance the infectivity of the HIV virus (3–5 orders of magnitude by some measures). To complement those studies, we performed in vitro assays of $PAP_{248-286}$, the most active precursor to SEVI, and other polycationic polymers to investigate the physical mechanisms by which the $PAP_{248-286}$ promotes the interaction with lipid bilayers. At acidic (but not at neutral) pH, freshly dissolved $PAP_{248-286}$ catalyzes the formation of large lipid flocculates in a variety of membrane compositions, which may be linked to the promotion of convective transport in the vaginal environment rather than transport by a random Brownian motion. Furthermore, $PAP_{248-286}$ is itself fusiogenic and weakens the integrity of the membrane in such a way that may promote fusion by the HIV gp41 protein. An α-helical conformation of $PAP_{248-286}$, lying parallel to the membrane surface, is implicated in promoting bridging interactions between membranes by the screening of the electrostatic repulsion that occurs when two membranes are brought into close contact. This suggests that nonspecific binding of monomeric or small oligomeric forms of SEVI in a helical conformation to lipid membranes may be an additional mechanism by which SEVI enhances the infectivity of the HIV virus.

INTRODUCTION

A puzzling discrepancy in AIDS research is the low in vitro activity of the virus compared to the explosive growth of the AIDS pandemic. It is estimated that AIDS has killed 25 million people since it was first recognized in 1981, making it one of the most destructive epidemics in human history. Yet the HIV virus is a surprisingly weak pathogen in vitro, with only a small percentage (0.1–.001%) of the virus particles able to replicate in vitro (1,2). Given the high rate of mutation of the HIV virus, it might seem reasonable to conclude that large numbers of structurally defective virus particles are produced, and only a small percentage of virus particles that are able to complete the steps of the virus life cycle are generated. Recent studies have shown that most virus particles are functional and, given the right opportunity, will infect their target cells (3). However, in contrast to the in vivo situation, in vitro conditions are such that most virus particles are never given the correct opportunity to attach and fuse with the target cell before the virus particle is degraded.

What is this critical difference between the in vivo and in vitro situations? HIV has an incredible ability to evolve quickly due to the high error rate of the viral reverse transcriptase. Given the HIV virus's ability to mutate rapidly, it also seems natural for the virus to exploit any available factors in the host environment that could be advantageous for infection. Because seminal fluid is ubiquitous during the sexual transmission of HIV, it is a likely source for cofactors that either inhibit or enhance the infectivity of the HIV virus (4–6). Despite the presence of seminal fluid in the vast majority of HIV infections, surprisingly little is known about the effects of semen on HIV infectivity (7–9). Although seminal fluid has been shown to enhance the binding of HIV virions to epithelial cells (9), the active component in enhancing the infectivity of HIV has only recently been identified. Fragments of prostatic acid phosphatase (PAP), a highly abundant protein found in human semen, act as a very dramatic enhancer of HIV infectivity. Fragments of PAP, named semen-derived enhancer of viral infection (SEVI; Fig. 1), were shown to strongly promote HIV virus-cell attachment and fusion in multiple viral and host cell genotypes at physiological concentrations (4). Most surprisingly, and most importantly, the SEVI peptide was found to drastically reduce the number of virus particles needed to establish infection under the low viral load conditions resembling sexual transmission. A truly remarkable enhancement of 4–5 orders of magnitude occurred when limiting amounts of virus were used. By comparison, most known endogenous enhancers had a much more modest 2–3-fold effect on the degree of HIV infectivity. In contrast to the large (and unrealistic) viral loads needed to infect cells in vitro, only 1–3 virus particles were necessary to establish a persistent infection in dendritic cells in the presence of SEVI (4). Notably, these assays detected spreading HIV-1 infection, implying that the detected virions were replication competent.

The mechanism by which SEVI enhances this remarkable enhancement of HIV infection is largely unknown. SEVI apparently has little effect on the transcription of viral RNA, as the reverse transcriptase inhibitor Efavirenz blocks viral gene expression in the presence of SEVI (4). However, SEVI drastically enhances viral binding and entry into cells,

Submitted June 11, 2009, and accepted for publication August 12, 2009.

*Correspondence: ramamoor@umich.edu or jbrender@umich.edu

Editor: Mark Girvin.

0006-3495/09/11/2474/10 $2.00

doi: 10.1016/j.bpj.2009.08.034

$PAP_{248\text{-}286}$ GIHKQKEKSRLQGGVLVNEILNHMKRATQIPSYKKLIMY
IAPP KCNTATCATQRLANFLVHSSNNFGAILSSTNVGSNTY-NH_2

FIGURE 1 Sequences of PAP248-286 and IAPP. (*Top row*) Sequence of PAP248-286. (*Bottom row*) Sequence of the control amyloidogenic peptide human IAPP. The C-terminus is amidated and a disulfide bond exists between Cys2 and Cys7.

enhancing HIV-1 viral fusion and subsequent gene expression ~10-fold (4). Furthermore, some degree of aggregation of the peptide is necessary for activity, since freshly prepared, monomeric solutions of SEVI are ineffective at promoting viral infectivity, and the enhancement of HIV infectivity increases with time as SEVI is incubated in solution. It has been established that SEVI is an amyloidogenic peptide, and that amyloid fibers of the peptide are more effective than the monomeric peptide in promoting HIV cell binding and membrane fusion (4). This is in agreement with previous studies that showed a more modest enhancement of infectivity of enveloped viruses by other amyloidogenic proteins, such as the Aβ peptide (10). However, the form of SEVI responsible was not clearly identified, as the rise in infectivity induced by SEVI preceded the formation of amyloid fibers (4).

Naturally occurring SEVI (the most active form of which is $PAP_{248\text{-}286}$) has a very large effect on the infectivity of the HIV virus. The physical mechanism by which it enhances the infectivity of HIV virus is not understood, but it has been hypothesized that amyloid fibers of SEVI physically capture entering virus particles and promote their interaction with the target cell membrane without bypassing the requirement for the appropriate cell receptor (4). The form of SEVI that is most active in this respect has not been identified, and the available data are somewhat inconclusive as regards the requirement for amyloid formation for enhancement of HIV infection. $PAP_{248\text{-}286}$ isolated in the monomeric form by size exclusion chromatography is ineffective at promoting HIV infection, and centrifugation of $PAP_{248\text{-}286}$ has shown that activity resides in the high-molecular-weight pellet rather than in the low-molecular-weight supernatant (4). However, time-dependent assays have shown that the infection-promoting activity of $PAP_{248\text{-}286}$ begins to increase well before amyloid formation occurs, as measured by β-sheet formation by circular dichroism (CD), Thioflavin T binding, or Congo red staining (4). In addition, the enhancement of infection shows up immediately when seminal fluid is spiked with freshly dissolved $PAP_{248\text{-}286}$ at pH 8.8, and within 30 min at pH 4.2 (4). Münch et al. (4) noted that the polycationic polymer Polybrene also promoted HIV infection (to a lesser degree than SEVI), a phenomenon that has also been noted for other retroviruses (11–14). The time-dependent results therefore suggest that an aggregated, but nonamyloid, form of $PAP_{248\text{-}286}$ can be as effective or even more effective than the fibrillar form of $PAP_{248\text{-}286}$ (4). These experiments were performed on in vivo systems, whose complexity complicates attempts to determine the physical basis for the interaction of SEVI with membranes. The use of simpler model membranes allows the dissection of physicochemical effects caused by the peptide, such as increased fusiogenicity and charge neutralization of the cellular membrane, from the effects on more complex properties such as cell viability and motility. The preliminary in vitro results shown here suggest that, under acidic conditions, freshly dissolved nonfibrillar $PAP_{248\text{-}286}$ appears to act similarly to other polycationic polymers, such as polybrene and polylysine, that act as general promoters of viral fusion (11–17).

MATERIALS AND METHODS

Lipid compositions of host and viral type membranes can be found in Aloia et al. (18) and in the Supporting Material. Details of vesicle preparation and CD spectroscopy can be found in Brender et al. (19) and in the Supporting Material. Further details about the materials and methods used in this study can be found in the Supporting Material.

RESULTS

Freshly dissolved $PAP_{248\text{-}286}$ promotes the aggregation of lipid vesicles

SEVI peptides have been proposed to increase the infectivity of HIV by increasing the attachment of virus particles to the cell membrane through charge neutralization. To compare the efficiency of $PAP_{248\text{-}286}$ with that of other cationic polymers, we performed turbidity assays for the aggregation of lipid vesicles induced by $PAP_{248\text{-}286}$, polybrene, and the amyloidogenic peptide human islet amyloid polypeptide (IAPP) (Fig. 2). The assays were performed at two different lipid concentrations to test the effects of the peptide/lipid ratio on vesicle aggregation. At this pH, none of the compounds induced substantial vesicle aggregation at a lipid concentration of 200 μM or 1000 μM. Polybrene, a highly charged cationic polymer commonly used to increase the efficiency of gene transfection, caused the most aggregation of the compounds tested (Fig. 2 *A*). Freshly dissolved human-IAPP, an amyloidogenic peptide with a charge of +3 at pH 7.3, caused slightly less aggregation. Significantly, freshly dissolved $PAP_{248\text{-}286}$ did not induce any aggregation at this pH, in agreement with the finding that freshly dissolved $PAP_{248\text{-}286}$ does not increase HIV infectivity and presumably does not increase the attachment of virus particles to the cell membrane.

The ability of SEVI to increase HIV infectivity has been linked to its cationic nature, since mutants in which the charged residues in $PAP_{248\text{-}286}$ are mutated to alanine form amyloid fibers but are not able to increase HIV infection rates (20). To check the influence of electrostatics on $PAP_{248\text{-}286}$ binding, we used an alternate lipid composition of 100% 1-palmitoyl-2-oleoyl-*sn*-glycero-3-phosphatidylglycerol (POPG; Fig. 2 *B*). The amount of lipid aggregation in this model membrane increased but was still less than has been reported for other amyloidogenic peptides (21).

The vaginal environment is typically acidic (near pH 4), and polycation-induced membrane aggregation and membrane fusion increase substantially near this pH as the pH approaches the pKa of the phosphatidylglycerol or

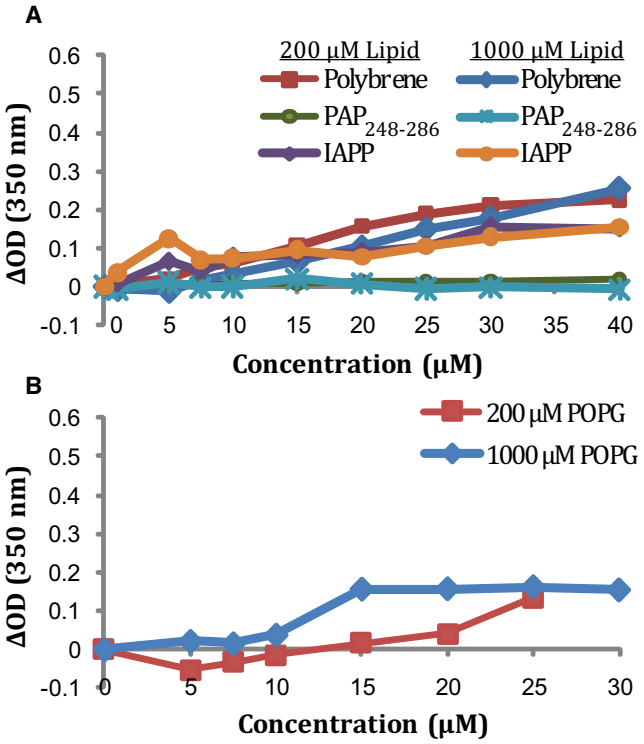

FIGURE 2 Lipid aggregation of liposomes detected by changes in turbidity at pH 7.3 (*A*) in the presence of POPC/POPG (7:3 ratio) vesicles and (*B*) POPG vesicles. Reported values are the changes in the absorbance at 350 nm relative to the control immediately after addition of the peptide or polymer and vigorous mixing. Two different lipid concentrations (200 μM and 1000 μM) were used as indicated.

phosphatidylserine headgroup (22–24). In addition, $PAP_{248-286}$ also has two His residues that are likely to be charged at pH 4 but not at pH 7.3, resulting in a higher electrostatic interaction with the membrane at pH 4. In contrast to the neutral pH condition, $PAP_{248-286}$ caused appreciable lipid aggregation at acidic pH in 7:3 1-palmitoyl-2-oleoyl-*sn*-glycero-3-phosphatidylcholine (POPC)/POPG liposomes (Fig. 3 *A*). Furthermore, the lipid aggregates produced are considerably larger than those produced at neutral pH and could be visibly detected sedimenting to the bottom of the cuvette, even under the influence of shaking or stirring (Fig. 3, *D* and *E*). Of interest, the decrease in pH had the opposite effect on human-IAPP, which caused more lipid aggregation than $PAP_{248-286}$ at neutral pH but did not cause any detectible lipid aggregation at pH 4. Similar results were obtained with membranes resembling the viral envelope (Fig. 3 *B*) and host cell (Fig. 3 *C*), albeit with a lesser degree of aggregation, most likely due to the decreased amount of anionic lipids or increased cholesterol content in these membranes.

Freshly dissolved $PAP_{248-286}$ promotes the mixing of lipid molecules between membranes in a manner suggestive of membrane fusion

In addition to promoting the binding of liposomes to each other, $PAP_{248-286}$ promotes the interchange of the membranes of both vesicles, as measured by a fluorescence probe dilution assay. Small unilamellar vesicles (SUVs) doubly labeled with rhodamine and NBD-labeled glycerophosphocholine probes (1% each) were mixed with unlabeled vesicles in the presence of the indicated concentrations of peptide. Fusion of the labeled vesicles with the unlabeled ones results in an increased average distance between probes and a decreased fluorescence resonance energy transfer (FRET) efficiency. Polylysine, polybrene, and $PAP_{248-286}$ all promoted the fusion of POPC/POPG SUVs in the absence of calcium (Fig. 4). In

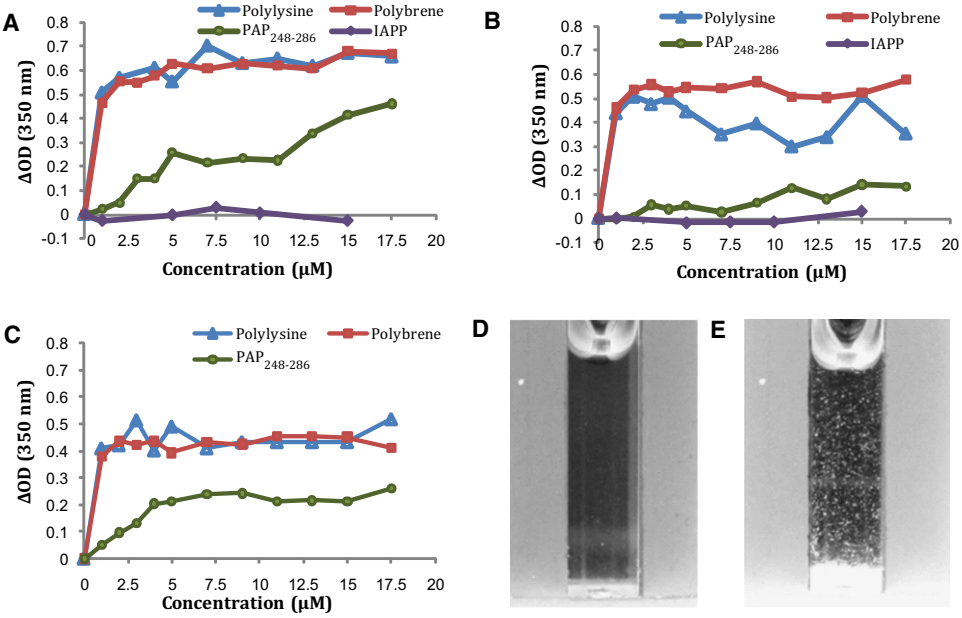

FIGURE 3 Lipid aggregation of liposomes of varying composition detected by changes in turbidity at pH 4: (*A*) 7:3 POPC/POPG, (*B*) viral membrane composition, and (*C*) host cell membrane composition. Reported values are the changes in the absorbance at 350 nm relative to the control immediately after addition of the peptide or polymer and vigorous mixing. (*D*) A photograph of the sample containing 100 nm 7:3 POPC/POPG liposomes at 500 μM concentration before the addition of 17.5 μM $PAP_{248-286}$. (*E*) A photograph of the same sample 10 min after the addition of 17.5 μM $PAP_{248-286}$.

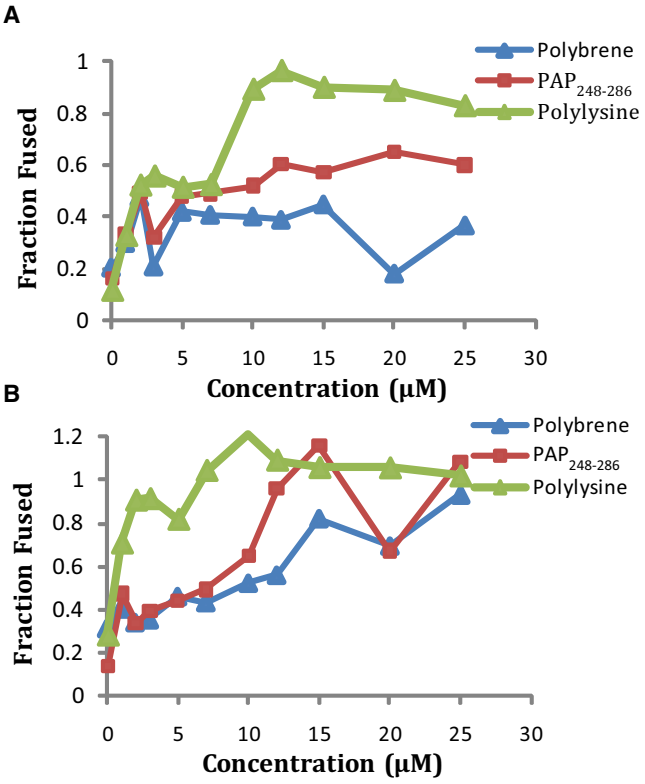

FIGURE 4 Membrane fusion induced at (*A*) pH 7.3 and (*B*) pH 4 by $PAP_{248\text{-}286}$ in 7:3 POPC/POPG vesicles as measured by a FRET-based lipid mixing assay. Samples were normalized to 100% lipid mixing using the FRET efficiency in the presence of 1% Triton-X.

contrast to vesicle aggregation, lipid mixing induced by low concentrations (<10 μM) of $PAP_{248\text{-}286}$ appears to be nearly as effective at neutral pH as at acidic pH. At higher concentrations (>12.5 μM) $PAP_{248\text{-}286}$ becomes as effective as polylysine at promoting the fusion of SUVs.

$PAP_{248\text{-}286}$ induces negative curvature in the membrane

The process of vesicle fusion is marked by the formation of a highly curved intermediate that is energetically unfavorable (25). Peptides that interact with the membrane in such a way as to reduce the physical stress imposed on the membrane by the formation of this highly curved intermediate can be expected to enhance fusion (26,27). The stabilization of membrane curvature by $PAP_{248\text{-}286}$ can be conveniently followed by recording the shift in the phase transition temperature from the flat liquid crystalline (L_α) phase to the highly curved inverted hexagonal phase (H_{II}) in which the lipid molecules are arranged cylindrically with the polar headgroups facing inward (26–30). Peptides that either stabilize negative (convex) membrane curvature or increase the bending elasticity of the membrane will favor the formation of the H_{II} phase, and will accordingly decrease the associated phase transition temperature (T_H) (31–34). DiPoPE has a T_H of 47.8°C under these conditions in the absence of $PAP_{248\text{-}286}$. The incorporation of $PAP_{248\text{-}286}$ into DiPoPE multilamellar vesicles reduced T_H (Fig. 5), indicating $PAP_{248\text{-}286}$ facilitates the formation of the highly curved H_{II} phase. The reduction of T_H with the incorporation of $PAP_{248\text{-}286}$ occurs as a two-step (or multiple-step) process. The incorporation of a very small percentage (0.00625 mol %) of $PAP_{248\text{-}286}$ into the DiPoPE vesicles led to a 0.9°C decrease in T_H, whereas larger percentages (0.25 and 0.4%) were required for further decreases in T_H. The reason for the multistage nature of the decrease in T_H is unclear at present.

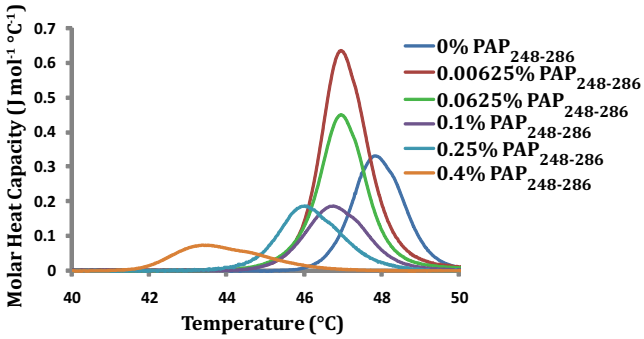

FIGURE 5 $PAP_{248\text{-}286}$ promotes the formation of the negatively curved inverted hexagonal (H_{II}) phase. DSC heating scans of DiPoPE multilamellar vesicless containing the listed molar %s of $PAP_{248\text{-}286}$.

Freshly dissolved $PAP_{248\text{-}286}$ induces membrane disruption

Many amyloid peptides are disruptive to membranes, and damage to the integrity of the cellular membrane is believed to be one of the main causes of amyloid-related pathologies. To see whether the $PAP_{248\text{-}286}$ peptide also possesses this prominent feature of amyloid peptides, we performed dye leakage experiments on POPG vesicles as a function of peptide concentration. Carboxyfluorescein is self-quenched if it is incorporated into the vesicle at high (40 mM) concentrations. Disruption of the integrity of the membrane of the vesicle by the peptide allows carboxyfluorescein to escape, reducing the effective concentration and eliminating the self-quenching effect, which can be normalized by total disruption of the vesicles by Triton-X. Fig. 6 shows the increase in fluorescence after the addition of $PAP_{248\text{-}286}$ to 100 μM POPG vesicles. The leakage of the dye carboxyfluorescein from large unilamellar vesicles upon the addition of $PAP_{248\text{-}286}$ indicates that $PAP_{248\text{-}286}$ induces significant membrane disruption if it binds to the membrane. $PAP_{248\text{-}286}$ did not induce significant disruption until a certain critical concentration (~500 nM) was reached. Membrane disruption in POPG vesicles increases sigmoidally beyond this critical concentration, reaching saturation at ~1.5 μM or a peptide/lipid molar ratio of 1.5%. However, in vesicles that more closely resemble the composition of either the viral lipid envelope (Fig. 6 *C*) or the host cell (Fig. 6 *B*), disruption

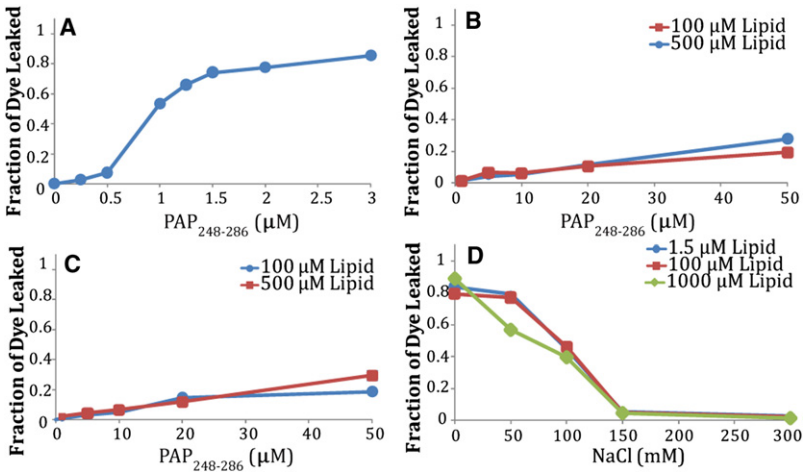

FIGURE 6 Membrane disruption caused by $PAP_{248-286}$ as measured by a dye leakage assay. Dye leakage assay as a function of $PAP_{248-286}$ concentration for 100 μM POPG vesicles (*A*), host-type vesicles by $PAP_{248-286}$ (*B*), and viral-type vesicles (*C*). (*D*) Dye leakage of the indicated concentrations of POPG vesicles by 1 μM $PAP_{248-286}$ as a function of NaCl concentration.

of the membrane is much less prominent. Although $PAP_{248-286}$ is very effective at permeabilizing POPG vesicles at nanomolar concentrations, even high peptide concentrations (50 μM) are insufficient for membrane disruption when the percentage of anionic lipids is lowered to levels that are typical of human cells.

The ability of $PAP_{248-286}$ to effectively disrupt POPG vesicles, but not vesicles with a lower anionic lipid content, suggests that electrostatic interactions form a large share of the free energy of membrane binding (35,36). To further investigate this possibility in model membrane systems, we recorded dye leakage from 7:3 POPG/POPC vesicles as a function of increasing salt concentration (Fig. 6 *D*). At the 150 mM NaCl concentration used in previous experiments, the membrane disruption induced by $PAP_{248-286}$ is negligible for this lipid system. However, when the NaCl concentration is lowered to 100 mM NaCl, there is significant membrane permeabilization, and the vesicles are almost entirely disrupted at 50 mM NaCl. This result, along with the polar and cationic nature of the peptide and the known correspondence between basic residues and the ability of $PAP_{248-286}$ to enhance HIV activity, suggests that the binding of $PAP_{248-286}$ to the membrane is primarily electrostatic in nature. However, the binding may be modulated by other factors, such as the degree of cholesterol incorporation into the membrane and the phospholipid type (37).

$PAP_{248-286}$ interacts weakly with the surface of lipid bilayers

The phase transition between the gel and liquid crystalline phases of lipids can be strongly perturbed by the binding of peptides to the membrane depending on the binding mode (38,39). The degree of perturbation is strongly dependent on the mode of binding. An amphiphilic peptide that partly penetrates into the interior of the membrane will interfere with lipid-lipid interactions within the membrane and therefore decrease the cooperativity of the phase transition, resulting in a decrease in the sharpness of the phase transition. Peptide binding at the water/membrane interface also disorders the surrounding lipids because the acyl chains of the lipid molecules must reorganize to fill the void created beneath the peptide in the hydrophobic core of the membrane, resulting in a decrease in the ΔH and phase transition temperature (T_m) associated with the transition. On the other hand, a peptide that is bound only to the surface of the membrane and does not penetrate into the interior of the membrane, or is bound in a transmembrane orientation will not have a significant effect on the phase transition because the lipid-lipid interactions are disrupted to a much lower degree compared to a surface-associated peptide (40).

Fig. 7 *A* shows the effect of $PAP_{248-286}$ on the phase transition of mixed 7:3 DMPC/DMPG vesicles as determined by differential scanning calorimetry (DSC). The DSC thermogram of pure 7:3 DMPC/DMPG vesicles shows a single main transition at 24.5°C indicative of the main gel-to-liquid crystalline phase transition, and a smaller pretransition at 5.4°C indicative of the rippled gel-to-gel phase transition (41). The addition of $PAP_{248-286}$ up to 2 mol % did not have a significant effect on the thermodynamics of the liquid crystalline-to-gel phase transition, except for a slight widening of the transition and a small shift of the transition to lower temperatures when the $PAP_{248-286}$ concentration exceeded 1 mol %. A similar effect was previously reported for low-molecular-weight polylysine. The absence of a significant effect suggests that the peptide is either peripherally bound to the surface of the membrane or is deeply inserted into the membrane in a transmembrane orientation, which would require less reorganization of the lipids to accommodate the peptide than a surface-bound orientation would. Although both types of binding would give rise to DSC thermograms similar to Fig. 7 *A*, a deep insertion into the membrane seems unlikely considering the high positive charge on the peptide and the lack of a hydrophobic or even amphipathic region in the peptide. Significantly, the main transition peak is nearly symmetrical at all concentrations of

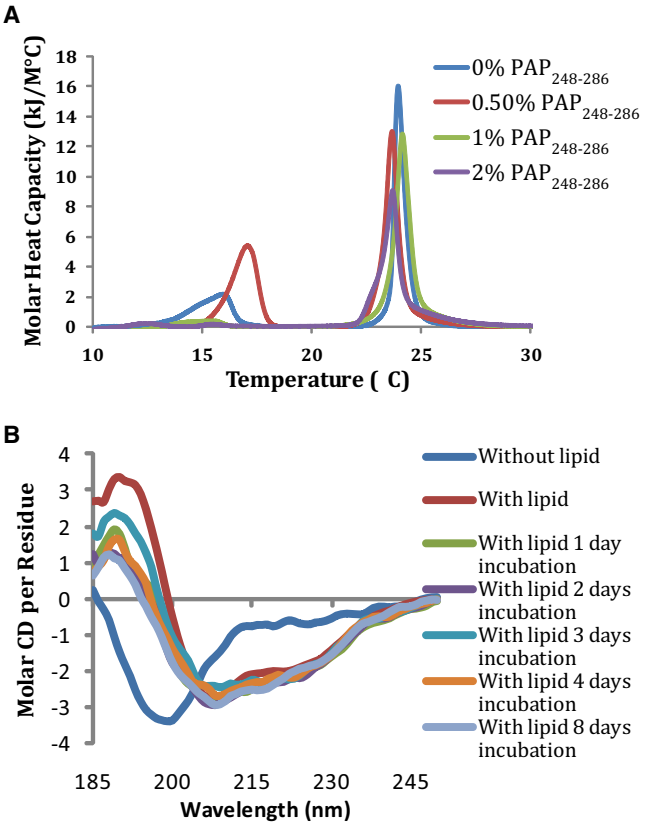

FIGURE 7 (*A*) Differential scanning calorimetry of the pretransition and the main gel-to-liquid crystalline phase transition of 7:3 DMPC:DMPG vesicles at the indicated $PAP_{248-286}$/lipid molar ratios. (*B*) CD spectra of 7 μM $PAP_{248-286}$ in 10 mM sodium phosphate buffer with 150 mM NaF at pH 7.3 as a function of incubation time after the addition of 1 mM 7:3 POPC/POPG vesicles.

$PAP_{248-286}$, indicating that $PAP_{248-286}$ does not induce domain formation in the membrane or phase separation of the sample, as has been observed for some rigid polycationic compounds and high-molecular-weight polylysines at higher mole percentages.

$PAP_{248-286}$ binds to membranes in a partial α-helical conformation

In addition to the random coil and amyloid β-sheet conformations found in solution, amyloid proteins frequently bind to membranes in α-helical conformations (42–44). The α-helical conformation represents an intermediate state before β-sheet aggregation and, perhaps paradoxically at first glance, is believed to catalyze the transition from the random coil conformation to the amyloid state (45). The α-helical conformation has been implicated as being responsible for the membrane-perturbing effects of many amyloid proteins. To see whether $PAP_{248-286}$ binds to lipid membranes in an α-helical conformation, we obtained CD spectra of $PAP_{248-286}$ incubated with 7:3 POPC/POPG liposomes (Fig. 7 *B*). The CD spectra show that freshly dissolved $PAP_{248-286}$ exists primarily in a random coil conformation, in agreement with previous findings. The addition of liposomes induces a conformational change in the peptide to a partial helical structure (Fig. 7 *B*). Analysis of the spectra shown in Fig. 7 *B* by the CONTINLL program suggests a helical content of ~30% (46); however, it is likely that this number underestimates the true helical content of the sample, as the signal from the peptide is apparently diminished at higher lipid concentrations where aggregation of the lipid vesicles is visible to the naked eye (see Fig. 3 *E*). An artificially low apparent concentration of $PAP_{248-286}$ tends to reduce the apparent conformational change upon lipid binding, because the simulated spectra constructed by the CONTINLL program compensates for the missing peptide signal by adding a random coil component of opposite sign. A comparison of $PAP_{248-286}$ with the crystal structure of the full PAP protein predicts two α-helices (residues 3–12 and residues 16–27) for $PAP_{248-286}$ separated by a flexible region containing the two glycines at positions 13 and 14 (47). Although $PAP_{248-286}$ is likely to adopt a different structure when bound to the membrane, the crystal structure of the full PAP protein does give an indication of the putative helical regions of membrane-bound $PAP_{248-286}$.

DISCUSSION

$PAP_{248-286}$ causes the formation of large lipid flocculates at acidic, but not neutral, pH

Freshly dissolved $PAP_{248-286}$ has a clear tendency to induce the aggregation of liposomes at acidic pH, but not at neutral pH, as indicated by the increase in optical density due to the higher scattering caused by larger aggregated liposomes. At neutral pH, none of the compounds tested, including the polycations polybrene and the amyloid peptides $PAP_{248-286}$ and human-IAPP, caused significant liposome aggregation. In fact, at neutral pH, $PAP_{248-286}$ had the least effect on liposome aggregation of all the compounds tested. At an acidic pH mirroring the vaginal environment before fertilization, the situation was quite different: $PAP_{248-286}$ and the polycationic polymer compounds caused significant aggregation at micromolar concentrations in partially anionic 7:3 POPC/POPG membranes and host-type membranes, and also in viral-type membranes to a somewhat smaller degree. Significantly, freshly dissolved human-IAPP, a strongly amyloidogenic peptide with a relatively high positive charge, did not strongly affect lipid aggregation. Furthermore, the lipid aggregates formed in this process were very large and rapidly fell out of solution and sedimented to the bottom.

The ability of $PAP_{248-286}$ to induce the formation of large lipid flocculates at acidic pH has interesting consequences if this result is confirmed in vivo. First, the presence of lipid aggregates confirms that $PAP_{248-286}$ interacts with model membranes, and, more importantly, has the ability to interact with two membranes simultaneously. Bridging interactions

between the viral and host cell membranes induced by monomeric or small oligomeric species of $PAP_{248-286}$ can enhance infection by enhancing viral binding to the cell. Second, the formation of large lipid aggregates may alter the mechanism of the initial approach of the virus to the cell surface. Detailed mechanistic studies have shown that the entry of retroviruses is ultimately limited by the diffusion of the virus to the target cell surface (48,49). Given enough time, all retrovirus particles will reach the appropriate receptor necessary to trigger fusion of the retrovirus with the target cell through Brownian motion. However, retroviruses are unstable in solution and have short half-lives (estimated to be on the order of ~6 h for free virions of HIV) that limit the available window of opportunity for infection (50). Brownian motion of the relatively small viral particle is inherently random and slow, and thus most virions are unable to reach the target cell surface before being destroyed. If viral particles aggregate together, the inefficient diffusion-limited capture process may be bypassed in favor of much more rapid sedimentation of the virus to the cell surface by convective processes (17). This process has been shown to be effective in promoting retrovirus infection in vitro, where directed mass transfer of the virus to plated cells significantly enhances infection rates (11,17,51–53). The effect of virus aggregation in the in vivo situation, where cell densities are much higher and target cells are in a three-dimensional matrix, is much less certain; however, the influence of $PAP_{248-286}$/SEVI on virus aggregation and convective transport warrants further investigation (54,55).

$PAP_{248-286}$ is fusiogenic and alters the physical properties of the membrane in a way that may favor fusion by gp41

In contrast to the formation of lipid flocculates, which can only be detected at acidic pH, $PAP_{248-286}$ causes lipid mixing at both neutral and acidic pH in the absence of calcium. Lipid mixing is one of the prerequisites for proper fusion of two membranes. In this instance, $PAP_{248-286}$ is more effective than polybrene but less effective than polylysine at both of the pH values tested. In addition to the direct promotion of fusion by $PAP_{248-286}$, binding of $PAP_{248-286}$ to the cell membrane changes the physical properties of the membrane in a way that may make it more susceptible to fusion by the gp41 protein of the HIV virus. Specifically, $PAP_{248-286}$ induces negative curvature in the membrane and disrupts lipid-lipid contacts, thus reducing the force needed by the HIV gp41 protein to rupture the membrane and promote fusion (56). Lastly, we have shown that $PAP_{248-286}$ can affect the membrane strongly enough to disrupt membrane integrity to allow the passage of small molecules (Fig. 6). This is an indication of a general weakening of the membrane structure induced by $PAP_{248-286}$. There is also an indication that such additions of additives that alter membrane structure may have such an effect on viral fusion. Pretreatment of cultured cells with phosphatidylserine, a fusion-promoting lipid, results in a relatively large increase (2- to 20-fold) in enveloped virus infection rates that is cumulative with the charge-shielding effect of polybrene (57). This effect has been linked to facilitation of the viral fusion process, because it occurs without a concomitant increase in viral binding to cells or virus receptor levels (57).

Role of a helical conformation of $PAP_{248-286}$ in lipid-bridging interactions

The CD spectra of $PAP_{248-286}$ bound to POPC/POPG vesicles suggest that $PAP_{248-286}$ binds initially to the membrane in a partial helical conformation, and that it can be stabilized at low concentration in this conformation for extended periods of time. This finding puts $PAP_{248-286}$ in the class of amyloid proteins that are essentially unstructured in solution but adopt α-helical conformations when initially bound to membranes (58,59). As helical conformations are also common early intermediates in the fibrillogenesis of amyloidogenic peptides, the binding of $PAP_{248-286}$ to the cellular membrane may be important for catalyzing the formation of SEVI from monomeric $PAP_{248-286.}$ (45,60) Although at first glance it might seem paradoxical that the stabilization of helical states of $PAP_{248-286}$ would promote the formation of an entirely different fold, the self-association of helical stretches in PAP_{248-28} can catalyze the amyloid formation by increasing the effective concentration of unfolded and aggregation-prone sequences within $PAP_{248-286}$ through the reduction of translational and rotational diffusion. This templating effect is partially responsible for the acceleration of fibrillogenesis of many amyloidogenic proteins by lipid membranes, helix-promoting solvents, and molecular crowding agents. Although the partially helical structure detected here was found to be stable only when bound to membranes, it may also represent a transient conformation of the peptide in solution. The CD spectra of $PAP_{248-286}$ in solution suggest a structure that is almost entirely in a random coil conformation; however, NMR studies have shown that other amyloidogenic peptides that appear unstructured by CD and FTIR transiently adopt helical structure (61,62).

A partially helical conformation of $PAP_{248-286}$ may also explain the fusiogenic activity of the peptide. In this α-helical conformation, the $PAP_{248-286}$ peptide can be expected to bind parallel to the surface of the bilayer, since a transmembrane orientation of the peptide is unlikely due to the difficulty in this orientation of simultaneously shielding all of the positively charged residues that radiate from the helix in all directions (see Fig. 8). A surface-associated helical conformation of $PAP_{248-286}$ has several features that make it an attractive model to explain the bilayer fusion induced by the monomeric form of the peptide. First, electrostatic binding of the peptide to the surface is likely to partially dehydrate the lipid headgroup, removing a steric barrier to fusion in a manner similar to that caused by the binding of polyethylene

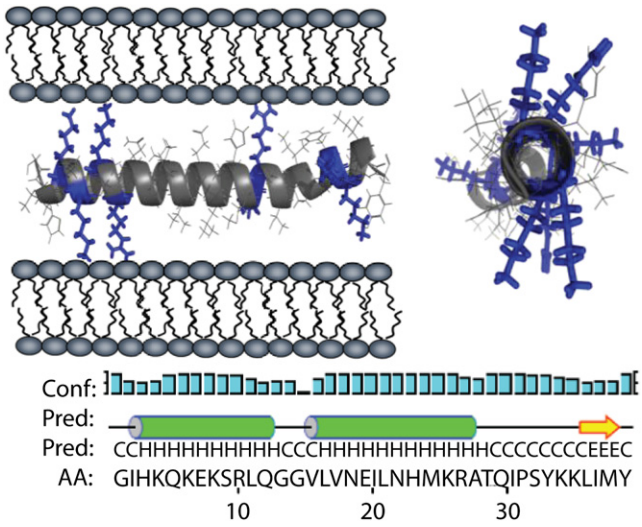

FIGURE 8 Two views of the proposed α-helical form of $PAP_{248-286}$ showing the radial distribution of positively charged residues and the possible interaction with the membrane. The secondary structure of $PAP_{248-286}$ within full-length PAP. The letter "C" represents a residue in the random coil conformation, "H" is a residue in a helical conformation, and "E" is a residue in the β-sheet conformation.

glycol (63). The removal of water from the lipid headgroup also has the effect of reducing the effective headgroup size of the lipid relative to the acyl chain. To compensate for this mismatch in relative sizes between the two regions of the lipid molecule, the membrane can curve outward, which is an obligate step for fusion that is strongly energetically unfavorable in the absence of $PAP_{248-286}$. Second, some of the lysine residues in this model face into the membrane, where they would interact with the lipid headgroups of the membrane, whereas other lysine residues face in the opposite direction into the aqueous phase. In this position, they are optimally positioned to diminish the long-range Coulombic repulsion that occurs when two bilayers of like sign are brought into contact. Furthermore, as the two bilayers approach each other during the initial stages of fusion, it is likely that the lysine chains of $PAP_{248-286}$ reach into the second bilayer to serve as an anchor linking the two bilayers together.

Since the structure of the amyloid form of $PAP_{248-286}$ is not known, it is difficult to make predictions about the possible membrane interactions of the amyloid form of $PAP_{248-286}$ as they are likely to be highly dependent on the supramolecular organization of the peptide. Notably, other amyloid proteins, which share the same gross cross-β sheet structure as the amyloid form of $PAP_{248-286}$, are less effective at promoting HIV infectivity (4). The determination of the high-resolution structure of the amyloid form of $PAP_{248-286}$ will likely be very informative in illuminating the nature of these differences.

CONCLUSIONS

Freshly prepared $PAP_{248-286}$ that is initially in the random coil conformation interacts strongly with lipid membranes, adopting a partial helical conformation that appears to promote bridging interactions between membranes and their eventual fusion by screening unfavorable electrostatic interactions. In this state, $PAP_{248-286}$ induces alterations in a variety of model membranes that appear to weaken lipid-lipid interactions and promote curved lipid phases that would be conducive to fusion. These alterations in membrane structure are not specific for the amyloid form of $PAP_{248-286}$ and are similar to changes in membrane structure produced by other disordered, polycationic polymers that also promote retroviral infection. The relative importance of the partially helical conformation for SEVI enhancement of HIV infection warrants further investigation. Given the very high degree of enhancement of HIV infectivity induced by SEVI, and its ubiquity in seminal fluid, such research is likely to have a high impact on investigations regarding HIV transmission and prevention.

SUPPORTING MATERIAL

Materials and methods are available at http://www.biophysj.org/biophysj/supplemental/S0006-3495(09)01394-0.

This study was supported by research funds from the National Institutes of Health (to A.R.).

REFERENCES

1. Dimitrov, D. S., R. L. Willey, H. Sato, L. J. Chang, R. Blumenthal, et al. 1993. Quantitation of human-immunodeficiency-virus type-1 infection kinetics. *J. Virol.* 67:2182–2190.
2. Rusert, P., M. Fischer, B. Joos, C. Leemann, H. Kuster, et al. 2004. Quantification of infectious HIV-1 plasma viral load using a boosted in vitro infection protocol. *Virology.* 326:113–129.
3. Thomas, J. A., D. E. Ott, and R. J. Gorelick. 2007. Efficiency of human immunodeficiency virus type 1 postentry infection processes: evidence against disproportionate numbers of defective virions. *J. Virol.* 81:4367–4370.
4. Münch, J., E. Rucker, L. Standker, K. Adermann, C. Goffinet, et al. 2007. Semen-derived amyloid fibrils drastically enhance HIV infection. *Cell.* 131:1059–1071.
5. Münch, J., L. Standker, K. Adermann, A. Schuz, M. Schindler, et al. 2007. Discovery and optimization of a natural HIV-1 entry inhibitor targeting the gp41 fusion peptide. *Cell.* 129:263–275.
6. Sabatte, J., A. Ceballos, S. Raiden, M. Vermeulen, K. Nahmod, et al. 2007. Human seminal plasma abrogates the capture and transmission of human immunodeficiency virus type 1 to cd4(+) t cells mediated by DC-Sign. *J. Virol.* 81:13723–13734.
7. Miller, C. J., and R. J. Shattock. 2003. Target cells in vaginal HIV transmission. *Microbes Infect.* 5:59–67.
8. Sharkey, D. J., A. M. Macpherson, K. P. Tremellen, and S. A. Robertson. 2007. Seminal plasma differentially regulates inflammatory cytokine gene expression in human cervical and vaginal epithelial cells. *Mol. Hum. Reprod.* 13:491–501.
9. Maher, D., X. Y. Wu, T. Schacker, J. Horbul, and P. Southern. 2005. HIV binding, penetration, and primary infection in human cervicovaginal tissue. *Proc. Natl. Acad. Sci. USA.* 102:11504–11509.
10. Wojtowicz, W. M., M. Farzan, J. L. Joyal, K. Carter, G. J. Babcock, et al. 2002. Stimulation of enveloped virus infection by β-amyloid fibrils. *J. Biol. Chem.* 277:35019–35024.

11. Landazuri, N., and J. M. Le Doux. 2004. Complexation of retroviruses with charged polymers enhances gene transfer by increasing the rate that viruses are delivered to cells. *J. Gene Med.* 6:1304–1319.
12. Davis, H. E., J. R. Morgan, and M. L. Yarmush. 2002. Polybrene increases retrovirus gene transfer efficiency by enhancing receptor-independent virus adsorption on target cell membranes. *Biophys. Chem.* 97:159–172.
13. Abe, A., A. Miyanohara, and T. Friedmann. 1998. Polybrene increases the efficiency of gene transfer by lipofection. *Gene Ther.* 5:708–711.
14. Arcasoy, S. M., J. D. Latoche, M. Gondor, B. R. Pitt, and J. M. Pilewski. 1997. Polycations increase the efficiency of adenovirus-mediated gene transfer to epithelial and endothelial cells in vitro. *Gene Ther.* 4:32–38.
15. Aubin, R. J., M. Weinfeld, and M. C. Paterson. 1988. Factors influencing efficiency and reproducibility of polybrene-assisted gene-transfer. *Somat. Cell Mol. Genet.* 14:155–167.
16. Bajaj, B., P. Lei, and S. T. Andreadis. 2001. High efficiencies of gene transfer with immobilized recombinant retrovirus: Kinetics and optimization. *Biotechnol. Prog.* 17:587–596.
17. Davis, H. E., M. Rosinski, J. R. Morgan, and M. L. Yarmush. 2004. Charged polymers modulate retrovirus transduction via membrane charge neutralization and virus aggregation. *Biophys. J.* 86:1234–1242.
18. Aloia, R. C., H. R. Tian, and F. C. Jensen. 1993. Lipid-composition and fluidity of the human-immunodeficiency-virus envelope and host-cell plasma-membranes. *Proc. Natl. Acad. Sci. USA.* 90:5181–5185.
19. Brender, J. R., E. L. Lee, M. A. Cavitt, A. Gafni, D. G. Steel, et al. 2008. Amyloid fiber formation and membrane disruption are separate processes localized in two distinct regions of IAPP, the type-2-diabetes-related peptide. *J. Am. Chem. Soc.* 130:6424–6429.
20. Roan, N. R., J. Münch, N. Arhel, W. Mothes, J. Neidleman, et al. 2009. The cationic properties of sevi underlie its ability to enhance human immunodeficiency virus infection. *J. Virol.* 83:73–80.
21. Kurganov, B., M. Doh, and N. Arispe. 2004. Aggregation of liposomes induced by the toxic peptides Alzheimer's a β s, human amylin and prion (106–126): facilitation by membrane-bound GM_1 ganglioside. *Peptides.* 25:217–232.
22. Tevi-Bénissan, C., L. Bélec, M. Lévy, V. Schneider-Fauveau, A. Si Mohamed, et al. 1997. In vivo semen-associated pH neutralization of cervicovaginal secretions. *Clin. Diagn. Lab. Immunol.* 4:367–374.
23. Lakhdarghazal, F., J. L. Tichadou, and J. F. Tocanne. 1983. Effect of pH and mono-valent cations on the ionization state of phosphatidylglycerol in monolayers—an experimental (surface-potential) and theoretical (Gouy-Chapman) approach. *Eur. J. Biochem.* 134:531–537.
24. Walter, A., C. J. Steer, and R. Blumenthal. 1986. Polylysine induces pH-dependent fusion of acidic phospholipid vesicles: a model for polycation-induced fusion. *Biochim. Biophys. Acta.* 861:319–330.
25. Chernomordik, L. 1996. Non-bilayer lipids and biological fusion intermediates. *Chem. Phys. Lipids.* 81:203–213.
26. Epand, R. M., and R. F. Epand. 1994. Relationship between the infectivity of influenza-virus and the ability of its fusion peptide to perturb bilayers. *Biochem. Biophys. Res. Commun.* 202:1420–1425.
27. Siegel, D. P., and R. M. Epand. 2000. Effect of influenza hemagglutinin fusion peptide on lamellar/inverted phase transitions in dipalmitoleoylphosphatidylethanolamine: Implications for membrane fusion mechanisms. *Biochim. Biophys. Acta.* 1468:87–98.
28. Hallock, K. J., D. K. Lee, and A. Ramamoorthy. 2003. MSI-78, an analogue of the magainin antimicrobial peptides, disrupts lipid bilayer structure via positive curvature strain. *Biophys. J.* 84:3052–3060.
29. Wildman, K. A. H., D. K. Lee, and A. Ramamoorthy. 2003. Mechanism of lipid bilayer disruption by the human antimicrobial peptide, LL-37. *Biochemistry.* 42:6545–6558.
30. Epand, R. F., I. Martin, J. M. Ruysschaert, and R. M. Epand. 1994. Membrane orientation of the SIV fusion peptide determines its effect on bilayer stability and ability to promote membrane-fusion. *Biochem. Biophys. Res. Commun.* 205:1938–1943.
31. Epand, R. M. 1998. Lipid polymorphism and protein-lipid interactions. *Biochim. Biophys. Acta.* 1376:353–368.
32. Israelachvili, J. N., S. Marcelja, and R. G. Horn. 1980. Physical principles of membrane organization. *Q. Rev. Biophys.* 13:121–200.
33. Cullis, P. R., and B. Dekruijff. 1979. Lipid polymorphism and the functional roles of lipids in biological-membranes. *Biochim. Biophys. Acta.* 559:399–420.
34. Gruner, S. M. 1989. Stability of lyotropic phases with curved interfaces. *J. Phys. Chem.* 93:7562–7570.
35. Bechinger, B., and K. Lohner. 2006. Detergent-like actions of linear amphipathic cationic antimicrobial peptides. *Biochim. Biophys. Acta.* 1758:1529–1539.
36. Ramamoorthy, A. 2009. Beyond NMR spectra of antimicrobial peptides: dynamical images at atomic resolution and functional insights. *Solid State Nucl. Magn. Reson.* 35:201–207.
37. Bechinger, B. 1999. The structure, dynamics and orientation of antimicrobial peptides in membranes by multidimensional solid-state NMR spectroscopy. *Biochim. Biophys. Acta.* 1462:157–183.
38. Pappalardo, G., D. Milardi, A. Magri, F. Attanasio, G. Impellizzeri, et al. 2007. Environmental factors differently affect human and rat IAPP: conformational preferences and membrane interactions of IAPP17–29 peptide derivatives. *Chem. Eur. J.* 13:10204–10215.
39. Grasso, D., D. Milardi, C. La Rosa, and E. Rizzarelli. 2001. Dsc study of the interaction of the prion peptide Prp106–126 with artificial membranes. *N. J. Chem.* 25:1543–1548.
40. McElhaney, R. N. 1986. Differential scanning calorimetric studies of lipid protein interactions in model membrane systems. *Biochim. Biophys. Acta.* 864:361–421.
41. Bayerl, T. M., T. Kochy, and S. Bruckner. 1990. On the modulation of a high-enthalpy pretransition in binary-mixtures of DMPC and DMPG by polar headgroup interaction. *Biophys. J.* 57:675–680.
42. Knight, J. D., J. A. Hebda, and A. D. Miranker. 2006. Conserved and cooperative assembly of membrane-bound α-helical states of islet amyloid polypeptide. *Biochemistry.* 45:9496–9508.
43. Jo, E. J., J. McLaurin, C. M. Yip, P. St George-Hyslop, and P. E. Fraser. 2000. α-Synuclein membrane interactions and lipid specificity. *J. Biol. Chem.* 275:34328–34334.
44. Terzi, E., G. Holzemann, and J. Seelig. 1997. Interaction of Alzheimer β-amyloid peptide(1–40) with lipid membranes. *Biochemistry.* 36:14845–14852.
45. Kirkitadze, M. D., M. M. Condron, and D. B. Teplow. 2001. Identification and characterization of key kinetic intermediates in amyloid β-protein fibrillogenesis. *J. Mol. Biol.* 312:1103–1119.
46. Greenfield, N. J. 2006. Using circular dichroism spectra to estimate protein secondary structure. *Nat. Protoc.* 1:2876–2890.
47. Jakob, C. G., K. Lewinski, R. Kuciel, W. Ostrowski, and L. Lebioda. 2000. Crystal structure of human prostatic acid phosphatase. *Prostate.* 42:211–218.
48. Tempaku, A. 2005. Random Brownian motion regulates the quantity of human immunodeficiency virus type-1 (HIV-1) attachment and infection to target cell. *J. Health Sci.* 51:237–241.
49. Chuck, A. S., M. F. Clarke, and B. O. Palsson. 1996. Retroviral infection is limited by Brownian motion. *Hum. Gene Ther.* 7:1527–1534.
50. Perelson, A. S., A. U. Neumann, M. Markowitz, J. M. Leonard, and D. D. Ho. 1996. HIV-1 dynamics in vivo: virion clearance rate, infected cell life-span, and viral generation time. *Science.* 271:1582–1586.
51. Landazuri, N., M. Gupta, and J. M. Le Doux. 2006. Rapid concentration and purification of retrovirus by flocculation with polybrene. *J. Biotechnol.* 125:529–539.
52. Landazuri, N., D. Krishna, M. Gupta, and J. M. Le Doux. 2007. Retrovirus-polymer complexes: study of the factors affecting the dose response of transduction. *Biotechnol. Prog.* 23:480–487.

53. Le Doux, J. M., N. Landazuri, M. L. Yarmush, and J. R. Morgan. 2001. Complexation of retrovirus with cationic and anionic polymers increases the efficiency of gene transfer. *Hum. Gene Ther.* 12:1611–1621.

54. Sturman, L. S., C. S. Ricard, and K. V. Holmes. 1990. Conformational change of the coronavirus peplomer glycoprotein at pH 8.0 and 37°C correlates with virus aggregation and virus-induced cell fusion. *J. Virol.* 64:3042–3050.

55. Hirst, G. K., and M. W. Pons. 1973. Mechanism of influenza recombination. 2. Virus aggregation and its effect on plaque formation by so-called noninfective virus. *Virology.* 56:620–631.

56. Harada, S., K. Yusa, K. Monde, T. Akaike, and Y. Maeda. 2005. Influence of membrane fluidity on human immunodeficiency virus type 1 entry. *Biochem. Biophys. Res. Commun.* 329:480–486.

57. Coil, D. A., and A. D. Miller. 2005. Enhancement of enveloped virus entry by phosphatidylserine. *J. Virol.* 79:11496–11500.

58. Jayasinghe, S. A., and R. Langen. 2005. Lipid membranes modulate the structure of islet amyloid polypeptide. *Biochemistry.* 44:12113–12119.

59. Abedini, A., and D. P. Raleigh. 2009. A role for helical intermediates in amyloid formation by natively unfolded polypeptides? *Phys. Biol.* 6:15005.

60. Knight, J. D., and A. D. Miranker. 2004. Phospholipid catalysis of diabetic amyloid assembly. *J. Mol. Biol.* 341:1175–1187.

61. Williamson, J. A., and A. D. Miranker. 2007. Direct detection of transient α-helical states in islet amyloid polypeptide. *Protein Sci.* 16:110–117.

62. Yonemoto, I. T., G. J. Kroon, H. J. Dyson, W. E. Balch, and J. W. Kelly. 2008. Amylin proprotein processing generates progressively more amyloidogenic peptides that initially sample the helical state. *Biochemistry.* 47:9900–9910.

63. Cevc, G., and H. Richardsen. 1999. Lipid vesicles and membrane fusion. *Adv. Drug Deliv. Rev.* 38:207–232.